

# High Frame Rate Vector Flow Imaging with a Convex Array in a simulated vessel phantom

Nina Ghigo<sup>1</sup>, Vincent Perrot<sup>1</sup>, Brahim Harbaoui<sup>1,2</sup>, Anne Long<sup>1,3</sup>,  
Stefano Ricci<sup>4</sup>, Piero Tortoli<sup>4</sup>, Didier Vray<sup>1</sup>, Hervé Liebgott<sup>1</sup>

<sup>1</sup>Univ. Lyon, INSA-Lyon, UCBL, UJM-Saint-Etienne, CNRS, Inserm, CREATIS UMR 5220, U1206, F-69621 Lyon, France

<sup>2</sup>Cardiology Department, European Society of Hypertension Excellence Center, Hopital de la Croix-Rousse et Hopital Lyon Sud, Hospices Civils de Lyon, Lyon, France

<sup>3</sup>Department of Internal Medicine and Vascular Medicine, Hospices Civils de Lyon, Hopital Edouard Herriot, Lyon, France

<sup>4</sup>Department of Information Engineering, Florence University, 50121 Florence, Italy

[nina.ghigo@creatis.insa-lyon.fr](mailto:nina.ghigo@creatis.insa-lyon.fr)

**Abstract**— In this paper, a flow estimation method based on transverse oscillation is applied, in high frame rate conditions, to the data collected using a convex array. All simulations were based on the transmission of the “natural” diverging wave due to the convex geometry of the probe when all elements are simultaneously excited. Transverse oscillation was introduced in the tangential direction in post-acquisition in the Fourier domain. Finally, 2D velocity vectors were extracted thanks to a phase-based estimator. Velocities were estimated with a bias of 8% of the peak velocity and a standard deviation lower than 7%. The method is now ready for experimental tests on flow phantoms and in vivo studies.

**Keywords**—flow, transverse oscillation, diverging wave, flow estimation, convex array

## I. INTRODUCTION

Cardiovascular diseases are known to induce modifications in artery properties such as elasticity, influencing the blood flow patterns and wall motions [1]–[3]. Ultrasound imaging is commonly used in hospitals to visualize blood vessels with frame rates typically below 100 images per second. Over the last two decades, ultrafast (high frame rate) imaging has been developed, allowing to produce more than 1000 images per second, depending on the depth of interest. This increased framerate allows the study of fast transient phenomena, and thus represents a powerful diagnosis tool [4].

In order to evaluate the health conditions of blood vessels a typical approach consists in measuring parameters related either to hemodynamics or to wall mechanics. These two aspects are usually studied separately even if wall and flow motions are inherently linked and should, therefore, be analyzed together. Several studies have been published on estimating the blood and tissues motion simultaneously using linear probes [5]–[10]. However, to the best of our knowledge, no similar results have been obtained using a convex probe.

Developing specific methods for convex probe geometry can be useful for the detection of cardiovascular diseases in vessels that are usually accessed by such probes. For example, aneurysm, a vascular disease characterized by a local increase in vessel diameter superior to 50%, develops in 80% of cases in the abdominal aorta. The presence of such disease induces

significant changes in wall mechanics and blood flow patterns [3]. The abdominal aorta is a deep artery and is therefore typically scanned with convex probes thanks to their relatively low frequency and large field of view.

Our final objective is to simultaneously estimate blood flow and tissue motion at high frame rate using a convex probe. This paper presents a preliminary study of the estimation of the 2D vector flow.

High frame rate vector flow imaging (HFR-VFI) produces detailed 2D velocity maps of medical interest like proven by the literature on carotid imaging using linear arrays. However, only a few studies present methods for using HFR-VFI with convex arrays. Either low frame rates are employed (< 100 fps, [11]) or contrast agents are used [12]. The transition from linear to convex geometry is not trivial, as all steps from beamforming to motion estimation must be suitably adapted to the convex geometry of the probe.

Transverse oscillation has been developed for flow estimation in 2D [13], [14]. Our group was among the first to combine the HFR transmission of plane waves with the use of transverse oscillation for HFR-VFI [15]. Transverse oscillation has been used by Jensen *et al* to access blood flow with a convex probe first in simulations [16] and then in livers *in vivo* but at a relatively low framerate (< 100 fps [11], [17], [18]). In this paper, we propose to combine transverse oscillation with diverging wave emission using a convex probe.

In the following section, the material and the transverse oscillation method in convex geometry are presented. Section III presents the results. Finally, Sections IV and V conclude the paper with a discussion of the results and a conclusion.

## II. MATERIAL AND METHOD

### A. Data acquisition

A straight vessel of 2 cm radius at 7 cm depth, with a laminar steady flow of 0.4 m/s peak velocity was simulated by Field II [19], [20]. The vessel was set perpendicular to the probe axis.

One naturally divergent wave (no delays in transmission, no compounding) was emitted at the pulse repetition frequency

(PRF) of 4 kHz with a convex array of similar properties as the C5-2 Philips probe. The acquisition parameters are detailed in Table I. Beamforming was achieved using a conventional delay-and-sum (DAS) algorithm with  $f_{\#} = 1$  in receive. The simulation was performed 20 times over different set of scatterers for repeatability evaluation.

TABLE I. ACQUISITION PARAMETERS

Probe pitch	424 $\mu\text{m}$
Probe number of elements	128
Probe radius of curvature	$R = 41.2 \text{ mm}$
Transmit frequency	$f_0 = 3.125 \text{ MHz}$
Sampling frequency	12.5 MHz
Transmit burst	5-cycle sinusoidal burst
Speed of sound	$c = 1540 \text{ m/s}$
Pulse repetition frequency	$PRF = 4000 \text{ Hz}$
Transmit apodization	Rectangular
Receive apodization	Rectangular
Number of simulations	20
Number of frames per simulation	20

### B. Flow estimation

Flow estimation was performed using the transverse oscillation technique. All following operations are carried out in the polar coordinate system of the probe since the point spread function (PSF) is invariant with angle in this domain. Interpolation over a Cartesian grid was used for visualization purpose only. Transverse oscillation is introduced in post-processing by multiplying the 2D Fourier spectrum of each RF image by a mask made of two Gaussians [21]. In this way, only the desired tangential wavelengths are preserved. The resulting Fourier spectrum is composed of four spots corresponding to the radial (natural) and tangential (introduced with the mask multiplication) frequencies. The natural radial oscillation due to ultrasound has a wavelength of  $\lambda_r = 0.25 \text{ mm}$ . Transverse oscillation was introduced with a wavelength of  $\lambda_\theta = 1.12^\circ$ , resulting in a wavelength of 1.8 mm at 5 cm depth (phantom starting depth) and of 2.6 mm at 9 cm depth (phantom ending depth) at the middle of the probe. The PSFs obtained after the transverse oscillation filtering in polar and Cartesian system are shown in Figure 1.

After this filtering, 2D analytical signals were extracted by selecting two different quadrants in the Fourier domain [22]. This technique assumes that the 2D oscillations now present in the RF images can be described as the product of two 1D oscillation signals. Each extracted analytic signal corresponds to one 1D oscillation signal and a phase base motion estimator can be used to recover motions. First, phase estimation is performed using a technique similar to the approach by Kasai *et al* [23] for the classic 1D case

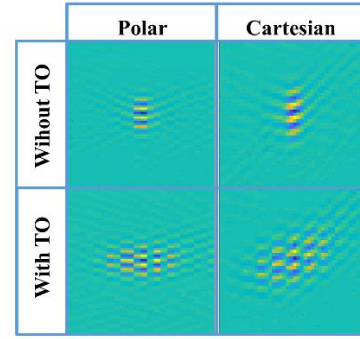


Figure 1: PSFs obtained at  $5^\circ$ , 5 cm radial distance, before and after transverse oscillation (TO) filtering, in polar and Cartesian coordinates; 2D oscillations can be seen after transverse oscillation filtering; PSF orientations are visible in Cartesian

$$\begin{cases} \phi_1(t) = \angle \sum_{t'=t-T/2}^{t+T/2} \hat{\mathcal{R}}_1(t') \\ \phi_2(t) = \angle \sum_{t'=t-T/2}^{t+T/2} \hat{\mathcal{R}}_2(t') \end{cases} \quad (1)$$

where  $\hat{\mathcal{R}}_1$  and  $\hat{\mathcal{R}}_2$  denote the complex autocorrelation function of the first and second quadrant analytic signal, respectively,  $\angle$  is the angle function and T the ensemble length. For each 20-frame long estimation, the ensemble length was set at  $T = 16$  frames. Spatial averaging was performed onto the complex autocorrelation estimates to reduce noise in the velocity estimation, a 2D rectangular window of size 1 mm ( $4\lambda_r$ ) per  $2.24^\circ$  ( $2\lambda_\theta$ ) was used. Here, the analytical signals extracted correspond to the two upper regions in the Fourier domain, i.e. to respectively the negative radial and negative tangential frequencies, and the negative radial and positive tangential frequencies. Then motion in the polar system was recovered from the phase shift

$$\begin{cases} v_r = \frac{-c \times PRF}{4\pi f_0} \times (\phi_1 + \phi_2) \\ v_\theta = \frac{-c \times PRF}{4\pi f_\theta} \times (\phi_1 - \phi_2) \end{cases} \quad (2)$$

where  $c$  is the speed of sound (m/s),  $f_0$  the transmit frequency (Hz) and  $f_\theta$  (degree $^{-1}$ ) the tangential frequency of the transverse oscillation. The radial velocity  $v_r$  and the tangential velocity  $v_\theta$  thus obtained are expressed in m/s and degree/s. The tangential motion is converted into m/s

$$v_\theta(i,j)_{m/s} = \sin(\theta_{(i,j)}) * (R + r_{i,j}) \quad (3)$$

where  $(i,j)$  denotes pixel coordinates and  $r_{i,j}$  the radial distance of such pixel. R is the radius of the convex probe.

The tangential and radial velocities are projected into axial  $v_x$  and lateral  $v_z$  velocities

$$\begin{cases} v_x(i,j) = v_r(i,j) \times \sin(\theta_{(i,j)}) + v_\theta(i,j) \times \cos(\theta_{(i,j)}) \\ v_z(i,j) = v_r(i,j) \times \cos(\theta_{(i,j)}) - v_\theta(i,j) \times \sin(\theta_{(i,j)}) \end{cases} \quad (4)$$

where  $\theta_{i,j}$  denotes the polar angle of the pixel of coordinates  $(i,j)$ .

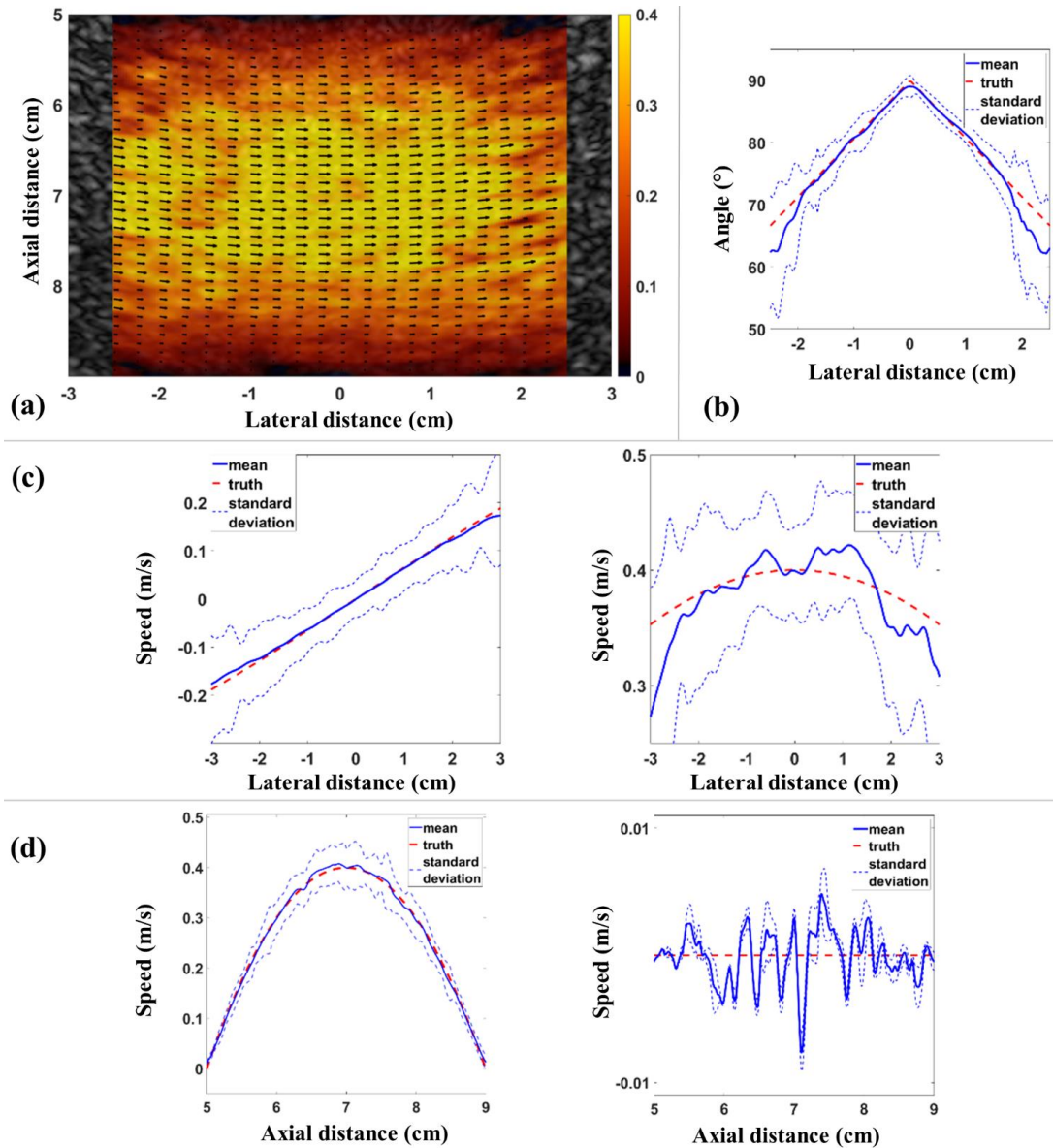


Figure 2: (a) Mean 2D flow velocity map of one of the simulated vessel phantom superimposed on its B-mode image; (b) Mean absolute angle between the ultrasound beam and the estimated blood flow for one simulation over the entire vessel height; (c) Mean radial (left) and tangential (right) velocities at the middle of the phantom ( $z = 7$  cm) in all simulations, the estimation loses in accuracy with the lateral distance due to loss of signals intensity and PSF orientation; (d) Mean axial (left) and lateral (right) velocities inside the vessel phantom over a 5 cm lateral field of view for all simulations, the residual axial estimate has a maximum absolute value lower than 0.01 m/s, the lateral velocity is estimated with an NRMSE lower than 5%.

### III. RESULTS

For visualization purpose, the estimated velocities were interpolated over a Cartesian grid. Results are shown Figure 2.

Figure 2 (a) shows the motion vectors superimposed to color-coded velocities over a 5 cm wide field of view (FOV) for one simulation. Figure 2 (c) shows the mean estimated radial (left) and tangential velocities (right) in the middle of the vessel in all simulations. As expected, the estimation is more accurate alongside the propagation of the ultrasound beams (radial direction) where the oscillations are naturally present. The

estimation accuracy is lower near the image edges due to a lack of signal and to the increase deformation of the PSF with the lateral distance. The FOV in which the tangential velocity can be estimated with a normal root mean square error (NRMSE) lower than 8% of the peak velocity is equal to 5 cm.

Figure 2 (d) shows the mean axial (left) and lateral (right) velocities over a 5 cm FOV for all simulations. Axial and lateral velocities are recovered from the radial and tangential velocities by using eq. (4). The axial blood velocity is correctly recovered with an NRMSE lower than 5% of the peak velocity. The residual axial estimate has a maximum absolute value lower than 0.01 m/s.

Figure 2 (b) shows the absolute angle between the ultrasound beam and the estimated blood flow for one simulation. The NRMSE is lower than 8% of the peak velocity over a 5 cm wide FOV.

#### IV. DISCUSSION

These results are encouraging, proving the ability of the method of estimating tangential and radial motions over a large FOV (5 cm) and up to a depth of 9 cm. The axial and lateral motions can be recovered accurately and easily understandable 2D velocity maps can be displayed (Figure 2 (a)). Nevertheless, this work is only preliminary and further studies are planned. The effect of clutter, which may yield tissue artifacts inside the vessel lumen, was not taken into account here. Since the final goal of this work is to simultaneously obtain tissue and blood motions, it could be interesting to use the information on tissue motion to create a temporal adaptive clutter filter [24] allowing more accurate blood flow estimation near the vessel walls. Tissue motion does not have the same properties as blood flow, therefore the parameters of the transverse oscillation and phase based motion estimator should be adapted accordingly.

#### V. CONCLUSION

In this paper, an imaging method able to detect the 2D blood flow pattern at 4 kHz frame rate using a convex probe has been presented. A phase-based motion estimator was used together with the transverse oscillation technique adapted to a divergent wave insonification. The results are promising and the estimated radial and tangential motions enable accurate recovery of axial and lateral motions. Velocity maps of the 2D blood flow can be displayed and have the potential to provide a useful visualization diagnostic tools for clinicians.

#### REFERENCES

- [1] M. E. Safar, B. I. Levy, and H. Struijker-Boudier, "Current Perspectives on Arterial Stiffness and Pulse Pressure in Hypertension and Cardiovascular Diseases," *Circulation*, vol. 107, no. 22, pp. 2864–2869, Jun. 2003.
- [2] P. Libby, "Inflammation and cardiovascular disease mechanisms," *The American Journal of Clinical Nutrition*, vol. 83, no. 2, pp. 456S–460S, Feb. 2006.
- [3] E. M. C. Kemmerling and R. A. Peattie, "Abdominal Aortic Aneurysm Pathomechanics: Current Understanding and Future Directions," in *Molecular, Cellular, and Tissue Engineering of the Vascular System*, vol. 1097, B. M. Fu and N. T. Wright, Eds. Cham: Springer International Publishing, 2018, pp. 157–179.
- [4] M. Tanter and M. Fink, "Ultrafast imaging in biomedical ultrasound," *IEEE Transactions on Ultrasonics, Ferroelectrics, and Frequency Control*, vol. 61, no. 1, pp. 102–119, Jan. 2014.
- [5] H. Hasegawa and H. Kanai, "Simultaneous imaging of artery-wall strain and blood flow realized by high frame rate acquisition of RF echoes," in *2008 IEEE Ultrasonics Symposium*, Beijing, China, 2008, pp. 225–228.
- [6] I. K. Ekroll, A. Swillens, P. Segers, T. Dahl, H. Torp, and L. Lovstakken, "Simultaneous quantification of flow and tissue velocities based on multi-angle plane wave imaging," *IEEE Transactions on Ultrasonics, Ferroelectrics and Frequency Control*, vol. 60, no. 4, pp. 727–738, Apr. 2013.
- [7] V. Perrot, H. Liebgott, A. Long, and D. Vray, "Simultaneous tissue and flow estimation at high frame rate using plane wave and transverse oscillation on in vivo carotid," p. 4, Oct. 2018.
- [8] P. Tortoli, T. Morganti, G. Bambi, C. Palombo, and K. V. Ramnarine, "Noninvasive simultaneous assessment of wall shear rate and wall distension in carotid arteries," *Ultrasound in Medicine & Biology*, vol. 32, no. 11, pp. 1661–1670, Nov. 2006.
- [9] Y. Wan, D. Liu, and E. S. Ebbini, "Imaging vascular mechanics using ultrasound: Phantom and in vivo results," in *2010 IEEE International Symposium on Biomedical Imaging: From Nano to Macro*, Rotterdam, Netherlands, 2010, pp. 980–983.
- [10] A. Ramalli *et al.*, "Continuous Simultaneous Recording of Brachial Artery Distension and Wall Shear Rate: A New Boost for Flow-Mediated Vasodilation," *IEEE Trans. Ultrason., Ferroelect., Freq. Contr.*, vol. 66, no. 3, pp. 463–471, Mar. 2019.
- [11] J. A. Jensen, A. H. Brandt, and M. B. Nielsen, "Convex array vector velocity imaging using transverse oscillation and its optimization," *IEEE Transactions on Ultrasonics, Ferroelectrics, and Frequency Control*, vol. 62, no. 12, pp. 2043–2053, Dec. 2015.
- [12] J. Voorneveld *et al.*, "High-Frame-Rate contrast-enhanced ultrasound for velocimetry in the human abdominal aorta," *IEEE Transactions on Ultrasonics, Ferroelectrics, and Frequency Control*, vol. 65, no. 12, pp. 2245–2254, Dec. 2018.
- [13] J. A. Jensen, "A new estimator for vector velocity estimation," vol. 48, no. 4, p. 9, 2001.
- [14] J. A. Jensen and P. Munk, "A new method for estimation of velocity vectors," *IEEE Transactions on Ultrasonics, Ferroelectrics and Frequency Control*, vol. 45, no. 3, pp. 837–851, May 1998.
- [15] M. Lenge, A. Ramalli, P. Tortoli, C. Cachard, and H. Liebgott, "Plane-wave transverse oscillation for high-frame-rate 2-D vector flow imaging," *IEEE Transactions on Ultrasonics, Ferroelectrics, and Frequency Control*, vol. 62, no. 12, pp. 2126–2137, Dec. 2015.
- [16] J. A. Jensen, "Optimization of transverse oscillating fields for vector velocity estimation with convex arrays," in *2013 IEEE International Ultrasonics Symposium (IUS)*, Prague, Czech Republic, 2013, pp. 1753–1756.
- [17] J. A. Jensen, Andreas Hjelm Brandt, and M. B. Nielsen, "In-vivo convex array vector flow imaging," in *2014 IEEE International Ultrasonics Symposium*, Chicago, IL, USA, 2014, pp. 333–336.
- [18] A. H. Brandt, K. L. Hansen, M. B. Nielsen, and J. A. Jensen, "Velocity estimation of the main portal vein with Transverse Oscillation," in *2015 IEEE International Ultrasonics Symposium (IUS)*, Taipei, Taiwan, 2015, pp. 1–4.
- [19] J. A. Jensen, "Field: A program for simulating ultrasound systems," presented at the 10th Nordic-Baltic Conference on Biomedical Imaging, 1996, vol. 34, pp. 351–353.
- [20] J. A. Jensen and N. B. Svendsen, "Calculation of pressure fields from arbitrarily shaped, apodized, and excited ultrasound transducers," *IEEE Trans. Ultrason., Ferroelect., Freq. Contr.*, vol. 39, no. 2, pp. 262–267, Mar. 1992.
- [21] S. Salles, A. J. Y. Chee, D. Garcia, A. C. H. Yu, D. Vray, and H. Liebgott, "2-D arterial wall motion imaging using ultrafast ultrasound and transverse oscillations," *IEEE Transactions on Ultrasonics, Ferroelectrics, and Frequency Control*, vol. 62, no. 6, pp. 1047–1058, Jun. 2015.
- [22] T. Bulow and G. Sommer, "Hypercomplex signals—a novel extension of the analytic signal to the multidimensional case," *IEEE Transactions on Signal Processing*, vol. 49, no. 11, pp. 2844–2852, Nov. 2001.
- [23] C. Kasai, K. Namekawa, A. Koyano, and R. Omoto, "Real-Time Two-Dimensional Blood Flow Imaging Using an Autocorrelation Technique," *IEEE Transactions on Sonics and Ultrasonics*, vol. 32, no. 3, pp. 458–464, May 1985.
- [24] V. Perrot *et al.*, "Spatial and Temporal Adaptive FIR Clutter Filtering," presented at the 2018 IEEE International Ultrasonics Symposium (IUS), Kobe, 2018, p. 4.